Journal of Catalysis 393 (2021) 281–289

Contents lists available at ScienceDirect

Journal of Catalysis

journal homepage: www.elsevier.com/locate/jcat

Versatile PNPO ligands for palladium and nickel catalyzed ethylene polymerization and copolymerization with polar monomers

Chen Zou [a,1], Daohong Liao [a,1], Wenmin Pang [a], Min Chen [b,*], Chen Tan [b,*]

[a] Department of Polymer Science and Engineering, Hefei National Laboratory for Physical Sciences at the Microscale, CAS Key Laboratory of Soft Matter Chemistry, University of Science and Technology of China, Hefei 230026, China

[b] Institute of Physical Science and Information Technology, Key Laboratory of Structure and Functional Regulation of Hybrid Materials of Ministry of Education, Anhui University, Hefei, Anhui 230601, China

ARTICLE INFO

Article history:
Received 22 September 2020
Revised 17 November 2020
Accepted 18 November 2020
Available online 30 November 2020

Keywords:
Olefin polymerization
Palladium
Nickel
PNPO ligand
Polar monomer

ABSTRACT

Asymmetric PO-type ligands are versatile platforms for palladium and nickel catalyzed ethylene polymerization as well as copolymerization of ethylene with polar monomers. In this work, a series of phosphinoamine phosphoramidate/phosphoramide ligands and the corresponding palladium/nickel catalysts were prepared, characterized and investigated in ethylene polymerization as well as copolymerization of ethylene with various polar monomers. The palladium and nickel complexes exhibited high activities in ethylene (co) polymerization, generating high-molecular-weight polyethylenes and copolymers of ethylene and polar monomers. The introduction of electron-donating substituents in the palladium catalytic system can significantly increase polymer molecular weights while maintaining high ethylene (co)polymerization activities. The less electronic donating substituents in the nickel catalysts led to increased catalytic activities in both ethylene polymerization and copolymerization with polar monomers. These results demonstrate the importance of ligand electronic effect in tuning the properties of nickel and palladium catalysts in ethylene polymerization and copolymerization reactions.

1. Introduction

Polyolefins have become the most common synthetic polymers, representing almost half of the plastics produced worldwide [1]. However, the non-polar nature of polyolefins limits their applications. The introduction of polar functional groups can not only improve important properties such as adhesion, compatibility and dyeability, but also provide a way to synthesize novel types of functional materials [2–11]. Compared with early transition metal catalysts, late transition metal catalysts exhibit lower oxophilicity. As a result, late-transition-metal catalyzed olefin copolymerization with polar monomers provides a direct and potentially economic route to access functionalized polyolefins [12–15]. For instance, Brookhart et al. discovered the α-diimine palladium and nickel catalysts in the 1990s (Chart 1, **A**) [16,17]. These catalysts exhibit high activities in ethylene polymerization, generating high molecular weight polyethylenes. Markedly, the α-diimine palladium catalyst can mediate olefin copolymerization with acrylates, vinylalkoxysilanes, and some comonomers bearing polar groups not directly attached to the C═C bond, affording branched polar functionalized polyolefins [18–34]. In 2002, Drent et al. reported that phosphine-sulfonate palladium catalysts can mediate the copolymerization of ethylene with alkyl acrylate (Chart 1, **B**) [35], generating linear copolymers. It was shown that this catalytic system is capable of copolymerizing ethylene with many challenging comonomers bearing polar groups directly attached to the C═C bond [36–44].

Since the electronic asymmetry of the P,O-type structure is believed to be critical for phosphine-sulfonate palladium catalyzed copolymerization [37,45,46], various ligands bearing both strongly and weakly σ-donating moieties have been developed subsequently. For example, the electronically asymmetric [P,P═O] cationic palladium catalysts (Chart 1, **C**) for olefin copolymerization with functionalized monomers were discovered by Nozaki and coworkers [47]. Chen and coworkers reported the phosphine phosphonic amide palladium catalysts (Chart 1, **D**). These catalysts are highly active in copolymerization of ethylene with polar functional monomers [48]. Carrow and coworkers reported an efficient phosphine phosphonic diamide palladium catalyst system (Chart 1, **E**), which is capable of copolymerizing of ethylene with polar monomers such as methyl acrylate, butyl acrylate, vinyl butyl ether and acrylic acid, generating high molecular weight copolymers

---

* Corresponding authors.
E-mail addresses: misschen@ahu.edu.cn (M. Chen), ctan@ahu.edu.cn (C. Tan).
[1] These authors contributed equally to this work.

https://doi.org/10.1016/j.jcat.2020.11.023
0021-9517/© 2020 Published by Elsevier Inc.

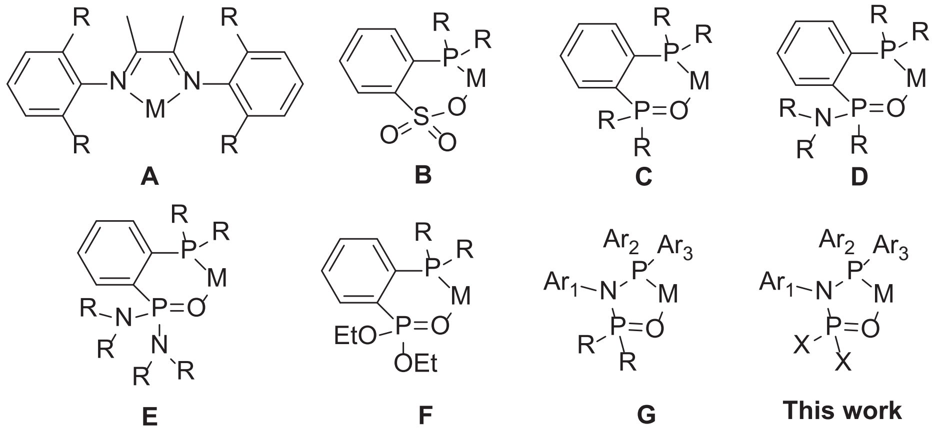

Chart 1. Selected palladium and nickel catalysts for olefin copolymerization with polar monomers.

[49]. Jordan and coworkers reported the studies of some phosphine phosphonate palladium catalysts (Chart 1, **F**). These catalysts can copolymerize ethylene with methyl acrylate and acrylic acid [50]. Recently, Chen and coworkers reported a versatile phosphinoamine phosphonic amide (PNPO) ligand platform. Both the palladium and nickel catalysts can catalyze ethylene copolymerization with polar monomers (Chart 1, **G**) [51,52]. It was envisaged that the combination of the ligand-rigidity effect [53,54], the bulky substituents, and the electronic-asymmetry nature of the [P,O]-type ligands enables the high-performances of this type of catalysts.

As part of our ongoing efforts in exploring the applications of versatile ligands for palladium and nickel catalyzed ethylene polymerization as well as copolymerization with polar monomers, we became interested in phosphinoamine-phosphoramidate and phosphinoamine-phosphoramide ligands (Chart 1, **This work**, X = NR_2 or OR type groups). It is hypothesized that these ligands bearing two amino/alkoxy groups on the P=O moiety could maintain the superior features of PNPO type ligands including bulky substituents, electronic-asymmetry and ligand-rigidity. Meanwhile, the installation of amino/alkoxy groups can provide additional flexibilities in tuning electronic natures of these ligands, since the $P(O)(NR_2)_2$ groups are more electronic donating while the $P(O)(OR)_2$ groups are less electronic donating compared with the $P(O)Ph_2$ group [Hammett constants: $P(O)(NMe_2)_2$, $\sigma_m = 0.30$; $P(O)Ph_2$, $\sigma_m = 0.38$; $P(O)(OMe)_2$, $\sigma_m = 0.42$] [55]. This subtle electronic effect could exert significant influences on the properties of these nickel and palladium catalysts in ethylene polymerization and copolymerization reactions.

2. Results and discussion

The ligands **L1**-**L3**, **L1′**-**L5′** can be easily prepared in a modular fashion in good yields (Scheme 1). The intermediates bearing piperidinyl, morpholino, diethylamino and alkoxy groups have been reported before [56–59]. The ligands **L1**-**L3** bearing two 2-$MeOC_6H_4$ groups ($Ar_1 = Ar_2$ = 2-$MeOC_6H_4$) and the ligands **L1′**-**L5′** bearing a sterically bulky biaryl substituent (Ar_1 = Ph, Ar_2 = 2-[2′,6′-$(MeO)_2$-C_6H_3]-C_6H_4) were synthesized. Subsequently, the palladium catalysts **Pd1**-**Pd3** were synthesized from the reaction of the ligands **L1**-**L3** with 1 equiv. (COD)PdMeCl in high yields. The complexes **Ni1**-**Ni5** were prepared from **L1′**-**L5′**, $[(allyl)NiCl]_2$ and sodium tetrakis(3,5-bis(trifluoromethyl)phenyl)borate (NaBAF) [51]. The ligands were characterized by ^1H NMR, ^{13}C NMR, ^{31}P NMR and electrospray ionization mass spectrometry (ESI-MS) analyses. The catalysts were characterized by ^1H NMR, ^{13}C NMR, ^{31}P NMR and elemental analyses. The catalysts **Pd-Ph** and **Ni-Ph** were previously reported, and prepared accordingly in this study for comparison purposes [51].

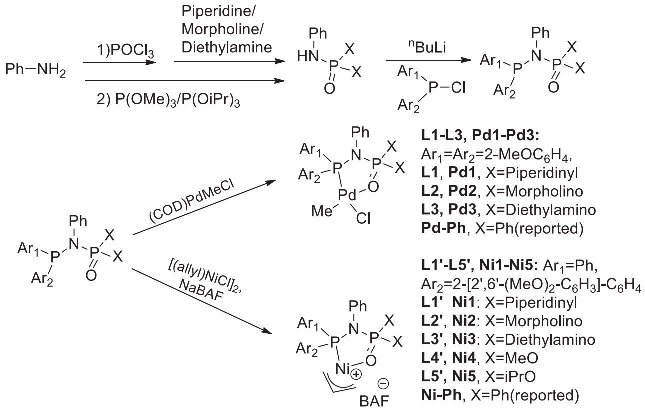

Scheme 1. Syntheses of ligands and catalysts.

Single crystals of complexes **Pd1** and **Ni3** were prepared from slow diffusion of Et_2O into a concentrated toluene solution. The molecular structures of **Pd1** and **Ni3** were determined by X-ray diffraction analysis (Fig. 1). The Pd or Ni center adopts a square planar geometry in each complex. The steric hindrance of the substituents on the phosphine moiety directly affects the steric environment around the Pd or Ni center. In contrast, the phosphine-oxide side is sterically open. For this type of palladium complexes, it was demonstrated that the smaller steric hindrance ($Ar_1 = Ar_2$ = 2-$MeOC_6H_4$) facilitates the insertion of polar monomers and polymerization activity without affecting the molecular weight of the polymer. In contrast, for nickel complexes, the steric hindrance associated with the bulky substituent (Ar_1 = Ph, Ar_2 = 2-[2′,6′-$(MeO)_2$-C_6H_3]-C_6H_4) can result in significantly increased activity and molecular weight of polyethylene [51]. Consequently, we designed the palladium complexes based on the small steric hindrance on the phosphorus and the nickel complexes with a bulky substituent on phosphorus. The ligand electronic effect was modulated through the substituents on the phosphorus oxygen side.

These palladium complexes exhibit high activities in ethylene homopolymerization by the activation of 1.2 eq. sodium tetrakis (3,5-bis(trifluoromethyl)phenyl)borate (NaBAF) (Table 1, entries 1–5). It was observed that **Pd3** resulted in the highest activity as well as the highest polyethylene molecular weight ($M_n = 8.8 \times 10^4$-

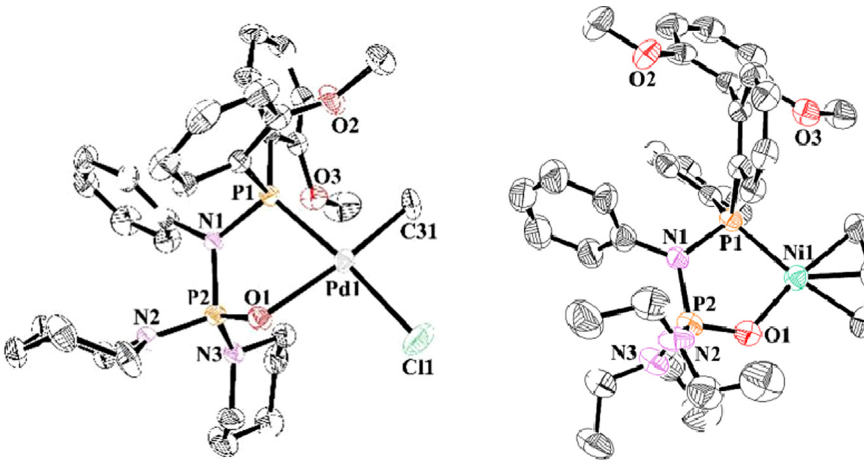

Fig. 1. Molecular structures of **Pd1** and **Ni3**. Hydrogen atoms and BAF were omitted for clarity. Selected bond distances (Å) and angles (deg) for: (left) **Pd1**: Pd1-P1 = 2.1959(14), Pd1-C31 = 2.031(5), Pd1-O1 = 2.268(4), Pd1-Cl1 = 2.3427(17); C31-Pd1-Cl1 = 91.10(18), O1-Pd1-P1 = 79.27(10); (right) **Ni3**: Ni1-P1 = 2.1894(18), Ni1-O1 = 1.875(5), Ni1-C35 = 1.984(7), Ni1-C36 = 1.949(9), Ni1-C37 = 2.005(8); C35-Ni1-C37 = 73.0(3), O1-Ni1-P1 = 90.11(14).

Table 1
Pd and Ni catalyzed ethylene homopolymerization.[a]

Ent.	Cat.	T(°C)	Yield(g)[b]	Act.(10^6)[b]	T_m (°C)[c]	M_n(10^4)[d]	M_w/M_n[d]
1	**Pd1**	80	2.1	1.1	134.8	3.2	5.9
2	**Pd2**	80	4.2	2.1	134.3	2.6	4.1
3	**Pd3**	60	0.3	0.2	137.1	8.8	4.3
4	**Pd3**	80	6.4	3.2	136.8	7.0	4.6
5	**Pd3**	100	3.1	1.6	134.4	3.0	4.7
6[e]	***Pd-Ph***	*80*	*5.0*	*2.5*	*128.7*	*1.4*	*3.3*
7	**Ni1**	80	0.9	0.2	124.7	1.4	1.8
8	**Ni2**	80	3.6	0.7	119.3	1.0	2.0
9	**Ni3**	80	0.3	0.06	127.5	1.6	2.4
10	**Ni4**	80	4.5	4.5	128.0	1.4	2.0
11	**Ni5**	80	1.6	1.6	126.4	1.4	2.0
12[e]	***Ni-Ph***	80	4.0	4.0	130.2	3.8	2.6

[a] Polymerization conditions: for Pd, catalyst = 2 μmol, 1.2 eq. NaBAF, toluene = 18 mL, CH_2Cl_2 = 2 mL, ethylene = 8 atm, 1 h; for Ni: **Ni1-Ni3** catalyst = 5 μmol, **Ni4-Ni5** catalyst = 1 μmol, toluene = 18 mL, CH_2Cl_2 = 2 mL, ethylene = 8 atm, 1 h.
[b] The yields and activities are average of at least two runs. Activity is in unit of 10^6 g·mol catalyst^{-1}·h^{-1}.
[c] Determined by differential scanning calorimetry (DSC).
[d] Determined by GPC in trichlorobenzene at 150 °C.
[e] Previously reported results.

g/mol) and melting point (137.1 °C). Temperature dependence studies showed that the molecular weight decreased with increasing temperature (Table 1, entries 3–5). Nevertheless, a relatively high polymer molecular weight (M_n = 3.0 × 10^4 g/mol) was achieved even at 100 °C, compared with the catalyst **Pd-Ph** (M_n = 1.4 × 10^4 g/mol at 80 °C). Moreover, the time-dependence studies show that **Pd3** remains highly active for 2 h at 100 °C (Fig. 2, A). It was indicated the catalyst **Pd3** exhibited higher thermal stability compared with **Pd-Ph** [51]. The catalyst **Pd3** decay more slowly than **Pd-Ph** at 100 °C (Figure S1, A). The Pd catalysts give high PDI values in ethylene polymerization. This is ascribed to the thermal instability of the PNPO-Pd catalysts during polymerization, since the formation of small amount of Pd(0) black formation was observed. Mecking et al. reported a relevant decomposition pathway in which the reductive elimination from the Pd hydride complexes lead to deactivation of catalysts as well as generation of Pd(0) [60].

Both **Pd1**, **Pd2** and **Pd3** resulted in higher molecular weight and melting point of polyethylene products compared with **Pd-Ph** [51]. This may result from the electronic effects. To provide a clear investigation on the electron-donating/withdrawing effects of substituents, computational studies based on density functional theory (DFT) calculations were performed. Here, the model molecules (**Pd1′**, **Pd2′**, **Pd3′**, and **Pd-Ph′**) were used (Scheme S1). It was indicated that the Mulliken charge values on the Pd centers follow the orders: **Pd1′** ≈ **Pd2′** ≈ **Pd3′** > **Pd-Ph′** (Table S1). Consequently, the $P(O)(NR_2)_2$ groups are more electronic donating compared with the $P(O)Ph_2$ group. Therefore, the introduction of electron-donating substituent groups in these palladium complexes is beneficial to significantly increase the melting point and molecular weight and maintain a relatively high ethylene polymerization activity, since electron-donating substituents could lead to increased electron density on the Pd center as well as decreased β-H transfer rate, resulting in improved molecular weight of polyethylene [30,41,61,62]. The catalyst **Pd3** led to higher molecular weights and activities than those of **Pd1** and **Pd2**. This could be due to the flexibility of the ethyl groups resulting in improved steric hindrance compared with the constrained cyclic groups [63,64].

The nickel complexes exhibited high activities (up to 4.5 × 10^6 g·mol^{-1}·h^{-1}) in ethylene polymerization in the absence of and cocatalysts or scaverngers at 80 °C (Table 1, entries 7–11), indicating they are potentially suitable for industrially used gas-phase ethylene polymerization conditions (80–100 °C) [65]. The activities of **Ni1**, **Ni2** and **Ni3** were much lower than those of **Ni-4** and **Ni-5** (Table 1, entries 7–11). Moreover, **Ni4** resulted in higher activity

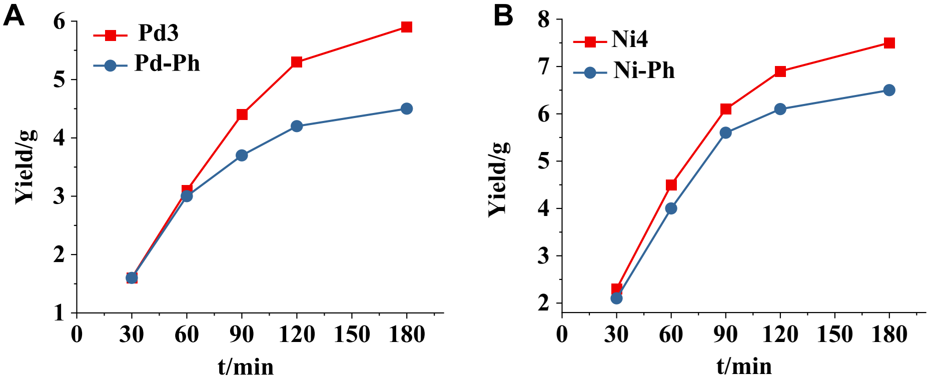

Fig. 2. (A) Plot of yield of polyethylene versus time (**Pd3** and **Pd-Ph**) (Conditions: **Pd3** and **Pd-Ph** 2 μmol, ethylene 0.8 MPa, CH_2Cl_2 2 mL, toluene 20 mL, 100 °C). **Pd-Ph**: reported. (B) Plot of yield of polyethylene versus time (**Ni4** and **Ni-Ph**) (Conditions: **Ni4** and **Ni-Ph** 2 μmol, ethylene 0.8 MPa, CH_2Cl_2 2 mL, toluene 20 mL, 80 °C). **Ni-Ph:** reported.

compared with **Ni5**. To investigate the influence of substituent electronic effects in Ni catalyzed ethylene polymerization, DFT calculations were performed. Herein, the model molecules (**Ni2′**, **Ni-Ph′**, **Ni4′**, and **Ni5′**) were used (Scheme S1). It was indicated that the Mulliken charge values on the Ni centers follow the orders: **Ni2′** > **Ni-Ph′** > **Ni5′** > **Ni4′** (Table S1). Consequently, the $P(O)(NR_2)_2$ groups are more electronic donating while the $P(O)(OR)_2$ groups are less electronic donating compared with the $P(O)Ph_2$ group. In addition, $P(O)(O^iPr)_2$ is less electronic donating compared with $P(O)(OMe)_2$. These results suggested that less electronic donating substituents in the nickel catalysts led to increased catalytic activities. It was suggested that the electron-withdrawing substituents can reduce of the electron density from the Ni center and lead to increased ethylene insertion rate associated with improved catalytic activity [41,66,67]. The catalyst **Ni-Ph** resulted in high activity and higher molecular weight of polyethylene compared with **Ni1**–**Ni5** (Table 1, entry 12). This may result from steric effects. The steric maps were generated by using the SambVca 2.1 A tool [68] (Figure S2). Here, the single crystal structure of the catalyst **Ni-Ph-OMe** (Scheme S2), a simulant of **Ni-Ph**, was used. It was indicated that the $\%V_{bur}$ (percentage of the sphere (r = 3.5 Å) around the metal occupied by ligand) of **Ni-Ph-OMe** (56.5) is about a fifth higher than that of Ni3 (48.0), indicating the catalysts **Ni-Ph-OMe** and **Ni-Ph** are sterically bulkier compared with **Ni3**. The time-dependence studies showed that **Ni4** remains highly active for 2 h at 80 °C (Fig. 2, B), and demonstrated similar thermal stability compared with **Ni-Ph** (Figure S1, B).

The palladium complexes **Pd1-Pd3** can mediate ethylene copolymerization with polar co-monomers such as methyl acrylate (MA), acrylic acid (AA) and allyl chloride, with moderate activities (up to 3.0×10^4 $g{\cdot}mol^{-1}{\cdot}h^{-1}$), affording copolymers with moderate molecular weights (M_n up to 1.03×10^4 Da), high copolymer melting temperatures (up to 118.0 °C) and high comonomer incorporation ratios (up to 9.3%) (Table 2). Most importantly, **Pd3** demonstrated much higher activity and copolymer molecular weights than those of **Pd-Ph** while maintaining similar level of comonomer incorporation. This further demonstrates the beneficial effects of electron-donating substituents in these palladium complexes.

The nickel complexes exhibited high activities (up to 1.8×10^5 $g{\cdot}mol^{-1}{\cdot}h^{-1}$) in ethylene copolymerization can copolymerize ethylene with a variety of polar monomers, including MA, 6-chloro-1-hexene, methyl 10-undecenoate, methyl 5-norbornene-2-carboxylaten and vinyltrimethoxysilane in the absence of any cocatalyst or protecting reagents (Table 3, entries 1–12). This is one of the very few single-component nickel catalyst systems that can copolymerize ethylene effectively with a variety of polar monomers affording copolymers with good co-monomer incorporation (1.0–4.2%) and moderate molecular weights (M_n up to 8.7×10^3 Da). The co-monomer incorporation ratios of the nickel complexes **Ni1-Ni5**, are higher than that of **Ni-Ph** in ethylene-MA copolymerization (Table 3, entry 6). This may result from steric effects (Figure S2). The nickel catalysts bearing electronic withdrawing $P(O)(OR)_2$ groups resulted in significantly increased activities compared with **Ni1**, **Ni2** and **Ni3** (Table 3, entries 4 versus 1–3; 7 versus 11; 10 versus 12). This further demonstrates the beneficial effects of electron-withdrawing substituents in this Ni catalytic system. The catalyst **Ni4** resulted in higher molecular weights than those of **Ni2**, probably due to the relatively lower incorporation ratios of polar monomers. The catalytic activities of **Ni4** were slightly higher than those of **Ni-Ph** in ethylene copolymerization with 6-chloro-1-hexene, methyl 10-undecenoate, methyl 5-norbornene-2-carboxylaten and vinyltrimethoxysilane (Table S2, entries 1–4), indicating their catalytic performance are similar in copolymerization of ethylene with special polar monomers bearing a spacer between the polar group and the double bond.

3. Experimental

3.1. General

All experiments were carried out under a dry nitrogen atmosphere using standard Schlenk techniques or in a glovebox. Deuterated solvents used for NMR spectroscopy were dried and distilled prior to use. ^1H, ^{13}C, ^{19}F, and ^{31}P NMR spectra were recorded on a Bruker AscendTm 400 spectrometer at ambient temperature unless otherwise stated. The chemical shifts of the ^1H and ^{13}C NMR spectra were referenced to tetramethylsilane, while the ^{31}P NMR spectra were referenced to an external 85% H_3PO_4 solution. Coupling constants are in Hz. Elemental analyses were performed by the Analytical Center of the University of Science and Technology of China. X-ray diffraction data were collected at 298 (2) K on a Bruker Smart CCD area detector with graphite-monochromated Mo Kα radiation (λ = 0.71073 Å). Molecular weights and molecular-weight distributions of the polymers were determined by gel permeation chromatography (GPC) using an Agilent PL-220 chromatograph equipped with two Agilent PLgel Olexis columns operating at 150 °C using o-dichlorobenzene as the solvent. The system was calibrated with a polystyrene standard and chromatograms were corrected for linear polyethylene through universal calibration using the Mark–Houwink parameters of Rudin: K = 1.75×10^{-2} cm^3/g and R = 0.67 for polystyrene, and K = 5.90×10^{-2} cm^3/g and R = 0.69 for polyethylene. Dichloromethane, THF, and

Table 2
Pd catalyzed copolymerization of ethylene with polar monomers.[a]

Ent.	Cat.	Comonomer	Yield(g)[b]	Act.(10^4)[b]	X_M (%)[c]	T_m (°C)[d]	M_n(10^3) [e]	PDI[e]
1	**Pd1**	MA	1.2	1.0	4.7	106.4	6.2	2.2
2	**Pd2**	MA	1.4	1.2	5.6	110.1	8.8	2.3
3	**Pd3**	MA	3.6	3.0	6.5	102.9	10.3	2.2
4[e]	***Pd-Ph***	*MA*	*2.0*	*1.7*	*6.8*	*100.6*	*6.1*	*2.5*
5	**Pd1**	AA	0.7	0.6	9.3	114.6	2.6	2.8
6	**Pd2**	AA	1.2	1.0	3.6	118.0	3.2	2.9
7	**Pd3**	AA	1.8	1.5	6.5	113.3	3.1	3.0
8[e]	***Pd-Ph***	*AA*	*0.9*	*0.8*	*6.3*	*112.6*	*2.8*	*2.9*
9	**Pd3**	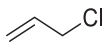	0.1	0.1	1.8	121.5	4.4	2.5

[a] Polymerization conditions: total volume of solvent and polar monomer (1 M/L) = 20 mL, catalyst = 20 μmol, ethylene = 8 atm, 80 °C, time = 6 h.

[b] The yields and activities are average of at least two runs. Activity is in unit of 10^4 g·mol^{-1}·h^{-1}.

[c] Determined by ^1H NMR in $C_2D_2Cl_4$ at 120 °C.

[d] Determined by DSC.

[e] Determined by GPC in trichlorobenzene at 150 °C. e Previously reported.

Table 3
Ni catalyzed copolymerization of ethylene with polar monomers.[a]

Ent.	Cat.	Comonomer	Yield(g)[b]	Act. (10^3)[b]	X_M (%)[c]	T_m (°C)[d]	M_n(10^3) [e]	PDI[e]
1	**Ni1**	MA	0.14	1.2	3.0	112.1	4.3	2.8
2	**Ni2**	MA	0.17	1.4	3.7	111.7	3.9	2.7
3	**Ni3**	MA	0.31	2.6	2.8	110.1	4.8	2.2
4	**Ni4**	MA	1.21	10.1	2.2	117.8	6.6	2.2
5	**Ni5**	MA	0.35	2.9	3.1	113.9	6.2	2.4
6	***Ni-Ph***	MA	0.7	5.8	2.1	123.0	9.9	2.2
7	**Ni4**	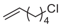	0.40	160.0	1.2	119.5	7.2	2.0
8	**Ni4**	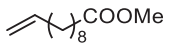	0.45	180.0	2.9	112.2	5.2	2.2
9	**Ni4**	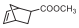	0.13	52.0	1.0	123.7	8.7	1.8
10	**Ni4**		0.43	72.0	2.4	118.3	7.0	1.9
11	**Ni2**	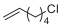	0.10	40.0	1.4	109.4	5.8	2.2
12	**Ni2**		0.13	52.0	4.2	103.7	4.5	2.7

[a] Polymerization conditions: total volume of solvent and polar monomer (1 mol/L) = 20 mL, Entry1-6: catalyst = 20 μmol, ethylene = 8 atm, 80 °C, time = 6 h. Entry 7–12:catalyst = 5 μmol, time = 30 min.

[b] The yields and activities are average of at least two runs. Activity is in unit of 10^4 g·mol^{-1}·h^{-1}.

[c] Determined by ^1H NMR in $C_2D_2Cl_4$ at 120 °C.

[d] Determined by DSC.

[e] Determined by GPC in trichlorobenzene at 150 °C.

hexanes were purified in solvent purification systems. The intermediates (*N*-Phenyl-*P*,*P*-di-1-piperidinylphosphinic amide, *P*,*P*-Di-4-morpholinyl-*N*-phenylphosphinic amide and *N*,*N*,*N*′,*N*′-Tetraethyl-*N*″-phenylphosphoric triamide) [52–55], PhArPCl and chlorobis(2-methoxyphenyl)phosphine [47] were prepared by literature procedures. Spectral data for [BAF]$^-$ counterion. The ^1H NMR resonances and ^{13}C NMR resonances of the [B-(3,5-$C_6H_3(CF_3)_2)_4]^-$ anion were the same for the different cationic nickel complexes and not repeated in the spectral data reported for each of the catalyst. ^1H NMR (400 MHz, $CDCl_3$) δ 7.75(s, 8H, *Hp* BAF), δ 7.53 (s, 4H, *Ho* BAF). ^{13}C NMR (101 MHz, $CDCl_3$) δ 161.90 (q, J_{CB} = 49.5 Hz, Cipso), 134.97 (s, Cp), 129.12 (q, J_{CF} = 31.5 Hz, Cm), 124.71 (q, J_{CF} = 272.5 Hz, CF_3), 117.65 (s, Co).

3.2. Ligand synthesis

Preparation of L1. *N*-Phenyl-*P*,*P*-di-1-piperidinylphosphinic amide (3.0 g, 10.0 mmol) was dissolved in dry THF (100 mL) under nitrogen and cooled to 0 °C, and ^{n}BuLi (2.5 M in hexane, 4 mL, 10.0 mmol) was added dropwise. The resulting solution was stirred for 12 h at room temperature after which chlorobis(2-methoxyphenyl)phosphine (2.8 g, 10.0 mmol) was added slowly at −78 °C. The mixture was stirred for another 24 h at room temperature after which it was evaporated to dryness under vacuum. The solid was dissolved in CH_2Cl_2 (200 mL) and filtered. The filtrate was evaporated to dryness under vacuum and the residue was washed with MeOH to yield a white solid (3.3 g, 56%). ^1H NMR (400 MHz, $CDCl_3$): δ 7.35–7.27 (br, 2H), 7.22 (t, *J* = 8.0 Hz, 2H), 7.07 (d, *J* = 8.0 Hz, 2H), 6.87 (t, *J* = 8.0 Hz, 2H), 6.85–6.75 (m, 3H), 6.73–6.67 (br, 2H), 3.68 (s, 6H), 3.25–3.05 (br, 8H), 1.55–1.38 (m, 8H), 1.37–1.28 (br, 4H). ^{31}P NMR ($CDCl_3$, 162 MHz): δ 44.9 (d, *J* = 70.4 Hz), 18.4 (d, *J* = 70.4 Hz). ^{13}C NMR (101 MHz, $CDCl_3$): δ 160.3 (s), 160.1 (s), 141.8 (d, J_{PC} = 6.0 Hz), 133.4 (d, J_{PC} = 3.0 Hz), 130.1 (s), 128.6 (d, J_{PC} = 2.0 Hz), 127.2 (s), 125.6 (d, J_{PC} = 3.0 Hz), 125.4 (d, J_{PC} = 3.0 Hz), 124.5 (s), 120.1 (s), 109.6 (s), 55.1 (s), 46.3 (s), 26.2 (d, J_{PC} = 2.0 Hz), 24.6(s). ESI-MS (*m*/*z*): [M+H]$^+$Calcd for $C_{30}H_{40}N_3O_3P_2$, 552.2545; Found: 552.2537.

Preparation of L2. Similar procedure as above **L1** was employed except *P*,*P*-Di-4-morpholinyl-*N*-phenylphosphinic amide (3.1 g, 10.0 mmol) was used. **L2** was obtained as a light white solid (2.7 g, 49%). ^1H NMR ($CDCl_3$, 400 MHz): δ 7.32–7.23 (m, 6H), 7.08 (d, *J* = 8.0 Hz, 2H), 6.92 (t, *J* = 8.0 Hz, 2H), 6.88–6.80 (m, 3H), 6.75–6.72 (m, 2H), 3.69 (s, 6H, *OMe*), 3.54–3.50 (m, 4H), 3.43–3.40 (m, 4H), 3.25–3.22 (m, 8H). ^{31}P NMR ($CDCl_3$, 162 MHz): δ 45.8 (d, J_{PP} = 69.5), 16.6 (d, J_{PP} = 69.5 Hz). ^{13}C NMR ($CDCl_3$, 101 MHz): 160.5(s), 160.3(s), 141.3(d), 133.3(s), 127.7(s), 124.9(s), 120.4(s), 110.0(s), 67.0(d), 55.2(s), 45.7(s). ESI-MS (*m*/*z*): [M+H]$^+$ Calcd for $C_{28}H_{36}N_3O_5P_2$, 556.2130; Found:556.2119.

Preparation of L3. Similar procedure as above **L1** was employed except *N*,*N*,*N*′,*N*′-Tetraethyl-*N*″-phenylphosphoric triamide (2.8 g, 10.0 mmol) was used. **L3** was obtained as a light white solid (2.1 g, 40%). ^1H NMR (400 MHz, $CDCl_3$) δ 7.29–7.23 (m, 2H), 7.14 (t, *J* = 7.8 Hz, 2H), 7.06 (d, *J* = 8.3 Hz, 2H), 6.79–6.70 (m, 5H), 6.64 (dd, *J* = 7.7, 5.0 Hz, 2H), 3.60 (s, 6H), 3.09 (m, 8H), 0.86 (t, *J* = 7.1 Hz, 12H). ^{31}P NMR ($CDCl_3$, 162 MHz): δ 43.33 (d, *J* = 79.6 Hz), 21.11 (d, *J* = 79.5 Hz). ^{13}C NMR (101 MHz, $CDCl_3$) δ

160.46 (s), 160.28 (s), 141.85 (d, J = 6.7 Hz), 133.51 (d, J = 3.8 Hz), 130.16 (s), 129.03 (d, J = 4.0 Hz), 127.06 (s), 126.12 (s), 125.87 (d, J = 4.2 Hz), 124.37 (s), 120.32 (s), 109.74 (s), 55.19 (s), 40.37 (t, J = 3.8 Hz), 14.18 (d, J = 2.7 Hz). ESI-MS (*m*/*z*): [M+H]$^+$ Calcd for C28H40N3O3P2, 528.2545; Found: 528.2534.

Preparation of L1′. *N*-Phenyl-*P*,*P*-di-1-piperidinylphosphinic amide (3.0 g, 10.0 mmol) was dissolved in dry THF (100 mL) under nitrogen and cooled to 0 °C, and ^{n}BuLi (2.5 M in hexane, 4 mL, 10.0 mmol) was added dropwise. The resulting solution was stirred for 12 h at room temperature after which **PhArPCl** (3.6 g, 10.0 mmol) was added slowly at −78 °C. The mixture was stirred for another 24 h at room temperature after which it was evaporated to dryness under vacuum. The solid was dissolved in CH_2Cl_2 (200 mL) and filtered. The filtrate was evaporated to dryness under vacuum and the residue was washed with MeOH to yield a white solid (3.8 g, 62%). ^{1}H NMR ($CDCl_3$, 400 MHz): δ 7.66–7.62 (m, 2H), 7.38–7.34 (m, 1H), 7.29–7.27 (m, 2H), 7.26–7.23 (m, 2H), 7.22–7.18 (m, 1H), 6.98–6.94 (m, 3H), 6.90–6.86 (m, 3H), 6.67 (d, J = 8.0 Hz, 1H), 6.55 (d, J = 8.0 Hz, 1H), 6.50–6.47 (m, 1H), 3.80 (s, 3H, *OMe*), 3.53 (s, 3H, *OMe*), 2.85–2.81 (m, 6H), 2.69–2.61 (m, 2H), 1.38–1.25 (m, 8H), 1.22–1.06 (m, 4H). ^{31}P NMR ($CDCl_3$, 162 MHz): δ 51.6 (d, J_{PP} = 87.3 Hz), 18.6 (d, J_{PP} = 87.3 Hz). ^{13}C NMR (100 MHz, $CDCl_3$):δ 157.8 (s), 157.7 (d, J_{PC} = 2.0 Hz), 142.3 (d, J_{PC} = 1.0 Hz), 142.0 (d, J_{PC} = 1.0 Hz), 141.6 (s), 141.2(s), 140.7 (d, J_{PC} = 6.0 Hz), 137.9 (m), 137.1 (s), 131.5 (s), 131.4 (s), 131.3 (d, J_{PC} = 3.0 Hz), 130.9 (d, J_{PC} = 7.0 Hz), 129.6 (s), 128.9 (s), 127.6 (s), 127.5 (s), 127.0 (d, J_{PC} = 2.0 Hz), 126.1 (s), 125.4 (s), 103.8 (d, J_{PC} = 6.0 Hz), 55.7 (s, *OMe*), 55.4 (s, *OMe*), 46.3 (s), 45.8 (m), 26.5 (d, J_{PC} = 5.0 Hz), 26.2 (d, J_{PC} = 5.0 Hz), 24.7 (d, J_{PC} = 14.0 Hz). ESI-MS (*m*/*z*): [M+H]$^+$ Calcd for $C_{36}H_{44}N_3O_3P_2$, 628.2852; Found: 628.2848.

Preparation of L2′. Similar procedure as above **L1′** was employed except *P*,*P*-Di-4-morpholinyl-*N*-phenylphosphinic amide (3.1 g, 10.0 mmol) was used. **L2′** was obtained as a light white solid (3.4 g, 55%). ^{1}H NMR ($CDCl_3$, 400 MHz): δ 7.64 (t, J = 8.0 Hz, 2H), 7.37 (t, J = 8.0 Hz, 1H), 7.33–7.27 (m, 3H), 7.25–7.20 (m, 2H), 7.05–6.96 (m, 3H), 6.90–6.81 (m, 3H), 6.68 (d, J = 8.0 Hz, 1H), 6.60 (d, J = 8.0 Hz, 1H), 6.46 (dd, J = 8.0 Hz, 4 Hz, 1H), 3.81 (s, 3H, *OMe*), 3.56 (s, 3H, *OMe*), 3.44–3.36 (m, 4H), 3.32–3.15 (m, 4H), 2.97–2.76 (m, 8H). ^{31}P NMR ($CDCl_3$, 162 MHz): δ 53.1 (d, J_{PP} = 81.5 Hz), 16.4 (d, J_{PP} = 81.5 Hz). ^{13}C NMR (101 MHz, $CDCl_3$): δ 157.37 (d, J_{PC} = 1.0 Hz), 157.6 (s), 141.6 (s), 141.1(d, J_{PC} = 12.0 Hz), 140.2 (d, J_{PC} = 7.0 Hz), 136.9 (s), 131.2 (s), 131.1 (s), 131.0 (s), 130.0 (s), 129.1 (s), 127.9 (s), 127.7 (d, J_{PC} = 3.0 Hz), 127.4 (s), 126.2 (s), 126.0 (s), 119.2 (d, J_{PC} = 7.0 Hz), 104.0 (d, J_{PC} = 9.0 Hz), 67.2 (d, J_{PC} = 5.0 Hz), 67.1 (d, J_{PC} = 5.0 Hz), 55.8 (s), 55.4 (s), 45.4 (s), 45.3 (d, J_{PC} = 7.0 Hz). ESI-MS (*m*/*z*): [M+H]$^+$ Calcd for $C_{34}H_{40}N_3O_5P_2$, 632.2443; Found: 632.2432.

Preparation of L3′. Similar procedure as above **L1′**was employed except *N*,*N*,*N′*,*N′*-Tetraethyl-*N″*-phenylphosphoric triamide (3.1 g, 10.0 mmol) was used. **L3′** was obtained as a light white solid (2.6 g, 43%). ^{1}H NMR (400 MHz, $CDCl_3$) δ 7.68–7.61 (m, 2H), 7.28 (td, J = 7.5, 1.1 Hz, 1H), 7.24–7.16 (m, 1H), 7.13–7.07 (m, 5H), 6.86 (s, 1H), 6.78 (td, J = 7.6, 1.3 Hz, 1H), 6.60 (d, J = 8.3 Hz, 1H), 6.49 (d, J = 8.3 Hz, 1H), 6.37 (dd, J = 7.5, 2.7 Hz, 1H), 3.73 (s, 3H, *MeO*), 3.49 (s, 3H *MeO*), 2.84–2.70 (m, 4H), 2.60 (dq, J = 10.1, 7.1 Hz, 4H), 0.80 (t, J = 7.1 Hz, 6H), 0.62 (t, J = 7.0 Hz, 6H). ^{31}P NMR (162 MHz, $CDCl_3$) δ 52.04 (d, J = 85.7 Hz), 20.79 (d, J = 85.7 Hz). ^{13}C NMR (101 MHz, $CDCl_3$) δ 156.94 (s), 156.82 (d, J = 1.4 Hz), 141.45 (s), 141.16 (s), 140.78 (s), 140.37 (s), 139.38 (d, J = 7.3 Hz), 137.48 (m), 136.48 (s), 130.56 (d, J = 3.3 Hz), 130.37 (s), 130.19 (s), 129.71 (d, J = 7.1 Hz), 128.69 (s), 127.89 (s), 126.55 (d, J = 2.7 Hz), 126.25 (s), 125.89 (d, J = 2.0 Hz), 125.21 (s), 124.22 (s), 118.63 (d, J = 7.3 Hz), 102.88 (s), 102.67 (s), 54.67 (s), 54.49 (s), 39.82 (dd, J = 8.1, 3.7 Hz), 39.30 (d, J = 3.5 Hz), 13.86 (s), 13.33 (d, J = 3.0 Hz). ESI-MS (*m*/*z*): [M+H]$^+$ Calcd for $C_{34}H_{44}N_3O_3P_2$, 604.2852; Found: 604.2847.

Preparation of L4. Weight 100 mmol of aniline in 250 mL of dichloromethane solution, add 50 mmol of trimethoxyphosphorus, add 20 mmol of iodine element, and after 12 h of reaction add 10 mL of 12 M hydrochloric acid, extract with $NaHCO_3$ and saturated NaCl solution successively, spin dry to obtain the product **1**.Under nitrogen protection, take 10 mmol of sample 1 dissolved in THF, add 1.1 eq of nBuLi dropwise at 0 °C, react for 2 h, add 10 mmol PhArPCl, after 12 h of reaction, extract, concentrate the organic phase and add ether to recrystallize a light white solid L4 (2.6 g, 43%). ^{1}H NMR (400 MHz, $CDCl_3$) δ 7.49 (dd, J = 10.3, 3.8 Hz, 2H), 7.36–7.30 (m, 1H), 7.31–7.17 (m, 4H), 7.04–6.95 (m, 3H), 6.92 (m, 1H), 6.88 (m, 2H), 6.83–6.74 (m, 1H), 6.64 (d, J = 8.3 Hz, 1H), 6.46 (d, J = 8.3 Hz, 1H), 3.80 (s, 3H, Ph*MeO*), 3.53 (d, J = 11.2 Hz, 3H), 3.45 (s, 3H, Ph*MeO*), 3.53 (d, J = 11.2 Hz, 3H). ^{31}P NMR (162 MHz, $CDCl_3$) δ 56.30 (d, J = 63.5 Hz), 8.92 (d, J = 63.5 Hz).^{13}C NMR (101 MHz, $CDCl_3$) δ 157.90 (s), 157.64 (d, J = 1.5 Hz), 141.77 (s), 141.37 (s), 140.48 (s), 140.28 (d, J = 3.1 Hz), 140.05 (d, J = 3.2 Hz), 136.25 (d, J = 4.8 Hz), 136.10 (d, J = 4.8 Hz), 135.28 (s), 131.54 (s), 131.36 (s), 131.05 (d, J = 6.8 Hz), 130.46 (d, J = 2.9 Hz), 129.91 (s), 129.22 (s), 128.32 (d, J = 1.2 Hz), 127.82 (d, J = 1.6 Hz), 127.78 (s), 127.74 (s), 126.48 (d, J = 1.6 Hz), 126.22 (s), 118.82 (d, J = 7.9 Hz), 103.89 (s), 103.54 (s), 55.80 (s), 55.38 (s), 54.05 (m), 53.95 (m). ESI-MS (*m*/*z*): [M+H]$^+$ Calcd for $C_{34}H_{44}N_3O_3P_2$, 522.1594; Found: 522.1601.

Preparation of L5. Similar procedure as above **L4** was employed except triisopropoxy phosphorus (2.89 g, 10.0 mmol) was used. **L5** was obtained as a light white solid (2.6 g, 43%).^{1}H NMR (400 MHz, $CDCl_3$) δ 7.45 (t, J = 6.7 Hz, 2H), 7.36 (td, J = 7.5, 1.3 Hz, 1H), 7.28–7.17 (m, 5H), 7.07 (dd, J = 7.4, 3.1 Hz, 1H), 7.04–6.94 (m, 4H), 6.92 (m, 2H), 6.64 (d, J = 8.4 Hz, 1H), 6.40 (d, J = 8.3 Hz, 1H), 4.34 (ddq, J = 25.2, 12.5, 6.3 Hz, 2H), 3.82 (s, 3H, *MeO*), 3.41 (s, 3H, *MeO*), 1.19 (dd, J = 6.0, 4.0 Hz, 6H, *MeOiPr*), 0.97 (d, J = 6.2 Hz, 3H, *MeOiPr*), 0.88 (d, J = 6.1 Hz, 3H, *MeOiPr*). ^{31}P NMR (162 MHz, $CDCl_3$) δ 55.17 (d, J = 57.1 Hz), 4.25 (d, J = 57.0 Hz). ^{13}C NMR (101 MHz, $CDCl_3$) δ 157.89 (s), 157.57 (d, J = 1.5 Hz), 141.57 (s), 141.45 (s), 141.05 (s), 140.42 (d, J = 3.2 Hz), 140.19 (d, J = 3.1 Hz), 136.98 (d, J = 4.4 Hz), 136.81 (d, J = 4.4 Hz), 135.05 (s), 132.07 (s), 131.88 (s), 130.88 (d, J = 6.4 Hz), 130.48 (dd, J = 3.0, 1.6 Hz), 129.55 (s), 129.07 (d, J = 19.6 Hz), 128.02 (d, J = 1.0 Hz), 127.60 (d, J = 1.4 Hz), 127.45 (d, J = 3.9 Hz), 126.23 (s), 125.97 (d, J = 1.3 Hz), 118.97 (d, J = 7.8 Hz), 104.08 (s), 103.34 (s), 72.18 (dd, J = 6.0, 1.8 Hz), 71.78 (d, J = 6.2 Hz), 55.97 (s), 55.26 (s), 23.85 (t, J = 3.8 Hz), 23.38 (d, J = 6.3 Hz), 23.26 (dd, J = 7.3, 2.1 Hz). ESI-MS (*m*/*z*): [M+H]$^+$ Calcd for $C_{34}H_{44}N_3O_3P_2$, 578.2220; Found: 578.2229.

3.3. Catalyst synthesis

Preparation of Pd1. A mixture of **L1** (551 mg, 1.0 mmol), (COD) PdMeCl (265 mg, 1.0 mmol) in 15 mL DCM was stirred at room temperature for 12 h. The resulting mixture was evaporated and the residual was washed by Et_2O (30 mL). The solid was collected by filtration to give **Pd1** as a light yellow solid (636 mg, 90%). ^{1}H NMR ($CDCl_3$, 400 MHz): δ 7.83–7.69 (br, 2H), 7.47 (t, J = 8.0 Hz, 2H), 7.16–7.09 (m, 3H), 6.97–6.87 (m, 6H), 3.49 (s, 6H, *OMe*), 2.93–2.78 (m, 8H), 1.51–1.39 (m, 12H). 0.45 (br, 3H, *Pd-Me*). ^{31}P NMR ($CDCl_3$, 162 MHz): δ 78.7 (d, J_{PP} = 61.2 Hz), 30.7 (d, J_{PP} = 61.2-Hz). ^{13}C NMR (101 MHz, $CDCl_3$) δ 160.73 (s), 141.07 (d, J = 7.9 Hz), 136.79 (s), 133.62 (s), 128.88 (s), 128.59 (s), 126.99 (s), 120.18 (d, J = 13.4 Hz), 118.50 (s), 117.97 (s), 111.32 (s), 55.42 (s), 46.21 (s), 25.88 (d, J = 5.0 Hz), 24.24 (s), −3.99 (s, *Pd-Me*). Anal. Calcd for $C_{31}H_{42}ClN_3O_3P_2Pd$: C, 52.55; H, 5.98; N, 5.93. Found: C, 52.42; H, 6.10; N, 5.90.

Preparation of Pd2. Similar procedure was employed except **L2** (555 mg, 1.0 mmol) was used. **Pd2** was obtained as a light yellow solid (611 mg, 86%). ^{1}H NMR (CDCl$_3$, 400 MHz): δ 7.78–7.65 (br, 2H), 7.51 (t, J = 8.0 Hz, 2H), 7.20–7.15 (m, 3H), 6.99–6.86 (m, 6H), 3.66–3.56 (m, 8H), 3.53 (s, 6H, *OMe*), 2.98–2.82 (m, 8H), 0.47 (d, J = 3.0 Hz, 3H, *Pd-Me*). ^{31}P NMR (CDCl$_3$, 162 MHz): δ 79.9 (d, J_{PP} = 63.2 Hz), 29.1 (d, J_{PP} = 63.2 Hz). ^{13}C NMR (101 MHz, CDCl$_3$) δ 160.83 (s), 140.71 (d, J = 7.6 Hz), 136.90 (s), 134.21 (s), 129.09 (s), 128.58 (s), 127.52 (s), 117.87 (s), 117.34 (s), 111.79 (d, J = 4.1 Hz), 66.81 (d, J = 4.2 Hz), 55.66 (s), 45.44 (s), −3.22 (s, *Pd-Me*). Anal. Calcd for $C_{29}H_{38}ClN_3O_5P_2Pd$: C, 48.89; H, 5.38; N, 5.90. Found: C, 48.58; H, 5.41; N, 5.92.

Preparation of Pd3. Similar procedure was employed except **L3** (613 mg, 1.0 mmol) was used. **Pd3** was obtained as a light yellow solid (527 mg, 75%). ^{1}H NMR (400 MHz, CDCl$_3$) δ 7.75 (dd, J = 13.8, 7.0 Hz, 2H), 7.46 (t, J = 7.7 Hz, 2H), 7.10–7.05 (m, 3H), 6.94 (t, J = 6.1 Hz, 4H), 6.88 (dd, J = 8.1, 5.0 Hz, 2H), 3.54 (s, 6H), 3.05–2.81 (m, 8H), 1.02 (t, J = 7.0 Hz, 12H), 0.46 (d, J = 3.0 Hz, 3H, *Pd-Me*). ^{31}P NMR (162 MHz, CDCl$_3$) δ 80.05 (d, J = 60.3 Hz), 33.94 (d, J = 60.3 Hz).^{13}C NMR (101 MHz, CDCl$_3$) δ 160.67 (d, J = 3.4 Hz), 141.02 (d, J = 7.3 Hz), 136.54 (s), 133.58 (s), 128.71 (s), 128.42 (s), 126.75 (s), 120.26 (d, J = 12.7 Hz), 118.48 (s), 117.94 (s), 111.33 (d, J = 4.5 Hz), 55.50 (s), 38.84 (d, J = 3.6 Hz), 13.04 (d, J = 3.6 Hz), −4.15 (s, *Pd-Me*). Anal. Calcd for $C_{29}H_{42}ClN_3O_3P_2Pd$: C, 50.89; H, 6.19; N, 6.14. Found: C, 50.67; H, 6.30; N, 6.21.

Preparation of Ni1. A mixture of **L1**′ (313 mg, 0.5 mmol), [Ni(allyl)Cl]$_2$ (67 mg, 0.25 mmol), and NaBAF (443 mg, 0.5 mmol) in 15 mL CH$_2$Cl$_2$ was stirred at room temperature for 12 h. The resulting mixture was filtrated and evaporated. The resulting solid was recrystallized from CH$_2$Cl$_2$ and hexanes solution to give **Ni1** as a bright yellow solid (1.2 g, 81%). ^{1}H NMR (CDCl$_3$, 400 MHz): δ 7.76–7.67 (m, 8H), 7.63–7.58 (m, 1H), 7.56–7.49 (m, 4H), 7.49–7.47(m, 1H), 7.43–7.27 (m, 5H), 7.24–7.13 (m, 6H), 6.94–6.86 (m, 1H), 6.69 (d, J = 8.0 Hz, 1H), 6.65–6.57 (m, 1H), 6.54–6.44 (m, 1H), 6.41 (d, J = 8.0 Hz, 0.5H), 5.70–5.55 (m, 0.5H), 4.55–4.42 (m, 0.5H), 4.23 (br, 0.5H), 4.09 (br, 0.5H), 3.66 (d, J = 4.0 Hz, 3H), 3.43 (d, J = 4.0 Hz, 3H), 3.21–2.90 (m, 4.5H), 2.75–2.54 (m, 4.5H), 2.30 (br, 1.5H), 1.67–1.14 (m, 12H), 1.11–1.08(m, 1H). ^{31}P NMR (CDCl$_3$, 162 MHz): δ 74.7 (d, J_{PP} = 71.0 Hz), 36.0 (d, J_{PP} = 71.0 Hz); δ 73.8 (d, J_{PP} = 77.4 Hz), 37.3 (d, J_{PP} = 77.4 Hz). ^{13}C NMR (101 MHz, CDCl$_3$) δ 161.47 (s), 160.97 (s), 160.47 (s), 159.98 (s), 156.86 (s), 135.72 (s), 133.81 (s), 132.52 (s), 132.40–132.13 (m), 131.46 (s), 131.16 (s), 130.79 (s), 129.54 (s), 129.28 (s), 128.37 (s), 128.08 (s), 127.52 (dd, J = 33.9, 20.1 Hz), 125.79 (s), 125.58–125.23 (m), 124.91 (s), 122.21 (s), 119.50 (s), 116.45 (s), 113.98 (d, J = 45.5 Hz), 103.84 (d, J = 35.8 Hz), 102.88 (s), 55.11 (d, J = 12.0 Hz), 54.39 (s), 47.23 (d, J = 29.9 Hz), 45.61 (d, J = 19.2 Hz), 45.09 (s), 24.92 (s), 24.41 (s), 22.77 (d, J = 12.3 Hz).

Preparation of Ni2. Similar procedure was employed except **L2**′ (316 mg, 0.5 mmol) was used. **Ni2** was obtained as a bright yellow solid (1.3 g, 86%). ^{1}H NMR (400 MHz, CDCl$_3$) δ 7.85–7.67 (m, 8H), 7.60 (s, 1H), 7.53 (s, 4H), 7.48 (s, 1H), 7.38 (s, 1H), 7.38–7.25 (m, 5H), 7.24–6.99(m, 6H), 6.65 (m, 2H), 6.50 (s, 0.5H), 6.41 (s, 1H), 5.66 (s, 0.5H), 4.56 (s, 0.5H), 4.31 (s, 0.5H), 4.09 (s, 0.5H), 3.63 (s, 6H), 3.44 (s, 2H), 3.40 (s, 6H), 3.04 (m, 4H), 2.76 (s, 4H), 2.48 (d, 1H), 1.49 (s, 0.5H), 1.26 (s, 0.5H). ^{31}P NMR (162 MHz, CDCl$_3$) δ 76.76 (dd, J = 212.1, 75.5 Hz), 36.99 (dd, J = 196.7, 75.0 Hz). ^{13}C NMR (101 MHz, CDCl$_3$) δ 161.78 (dd, J = 99.5, 49.9 Hz), 157.76 (s), 136.08 (s), 134.35 (s), 132.65 (d, J = 23.8 Hz), 132.32 (s), 130.54 (s), 130.10 (d, J = 24.2 Hz), 129.78 (s), 129.27 (d, J = 31.0 Hz), 128.86–128.18 (m), 127.06 (s), 125.98 (s), 123.27 (s), 120.56 (s), 118.36 (s), 117.51 (s), 115.47 (s), 105.11 (d, J = 39.8 Hz), 104.20 (s), 73.38–73.02 (m), 66.31 (dd, J = 26.7, 4.8 Hz), 56.20 (s), 55.42 (s), 48.72 (s), 45.68 (s), 45.23 (s).

Preparation of Ni3. Similar procedure was employed except **L3**′ (302 mg, 0.5 mmol) was used. **Ni3** was obtained as a bright yellow solid (1.2 g, 77%). H NMR (CDCl$_3$, 400 MHz): δ 7.74–7.63 (m, 8H), 7.62–7.57 (m, 1H), 7.55–7.54 (m, 1H), 7.53–7.46 (m, 4H), 7.38–7.27 (m, 4H), 7.24–7.11 (m, 7H), 6.89 (t, J = 8.0 Hz, 1H), 6.69 (d, J = 8.0 Hz, 1H) 6.63–6.56 (m, 1H), 6.50 (t, J = 8.0 Hz, 1H), 6.40 (d, J = 8.0 Hz, 0.5H), 5.62–5.53 (m, 0.5H), 4.51–4.44 (m, 0.5H), 4.22–4.18 (m, 0.5H), 4.07–4.02 (br, 0.5H), 3.66 (d, J = 2.0 Hz, 3H), 3.42 (d, J = 8.0 Hz, 3H), 3.19–3.10 (m, 2H), 3.05–2.94 (m, 2H), 2.81–2.68 (m, 4H), 2.55 (dd, J = 14.0 Hz, 614.0 Hz, 0.5H), 2.30–2.28 (br, 0.5H), 2.27–2.21 (br, 0.5H), 1.11 (t, J = 8.0 Hz, 3H), 1.05 (t, J = 8.0 Hz, 3H), 0.90–0.76 (m, 6H). ^{31}P NMR (CDCl$_3$, 162 MHz): δ 75.4 (d, J_{PP} = 72.1 Hz), 40.3 (d, J_{PP} = 72.1 Hz); δ 74.9 (d, J_{PP} = 78.4-Hz), 41.7 (d, J_{PP} = 78.4 Hz). ^{13}C NMR (101 MHz, CDCl$_3$) δ 160.74 (dd, J = 99.7, 49.9 Hz), 157.02 (dd, J = 24.0, 17.0 Hz), 139.36 (t, J = 20.0 Hz), 136.00 (s), 133.83 (s), 132.44 (dd, J = 18.5, 9.2 Hz), 131.40 (s), 131.28 (d, J = 4.4 Hz), 131.15 (s), 130.81 (s), 129.74 (s), 129.56 (s), 129.24 (s), 128.35 (s), 128.09 (s), 127.81 (s), 127.64 (s), 127.56 (s), 127.46 (s), 127.32 (s), 127.21 (s), 125.65 (d, J = 8.1 Hz), 125.31 (d, J = 7.2 Hz), 124.94 (s), 122.23 (s), 119.52 (s), 116.46 (s), 114.00 (d, J = 60.5 Hz), 103.99 (d, J = 36.4 Hz), 102.95 (s), 71.55 (d, J = 21.1 Hz), 55.35 (d, J = 10.4 Hz), 54.35 (s), 47.17 (d, J = 19.8 Hz), 39.08 (s), 38.58 (s), 12.40 (s), 12.24 (d, J = 2.9 Hz), 12.15 (s).

Preparation of Ni4. Similar procedure was employed except **L4** (302 mg, 0.5 mmol) was used. **Ni4** was obtained as a bright yellow solid (1.2 g, 77%) ^{1}H NMR (400 MHz, CDCl$_3$) δ 7.78 (s, 8H), 7.63 (s, 2H), 7.58 (s, 4H), 7.51 (s, 5H), 7.33 (t, J = 12.7 Hz, 2H), 7.22 (t, J = 7.6 Hz, 2H), 7.07 (s, 1H), 6.90 (s, 3H), 6.80 (s, 1H), 6.72 (s, 0.5H), 6.51 (s, 1H), 5.41 (s, 0.5H), 4.26 (s, 1H), 4.03 (m, 3H), 3.75 (s, 6H), 3.51 (s, 3H), 3.09 (s, 0.5H), 2.42 (s, 0.5H), 2.13 (s, 0.5H), 1.85 (s, 0.5H), 1.32 (s, 0.5H), 1.12 (s, 0.5H), 0.89 (m, 1H). ^{31}P NMR (162 MHz, CDCl$_3$) δ 73.27 (d, J = 96.9 Hz), 23.12 (dd, J = 215.8, 93.4 Hz). ^{13}C NMR (101 MHz, CDCl$_3$) δ 161.74 (dd, J = 99.7, 49.9 Hz), 135.53 (s), 134.82 (s), 133.87 (d, J = 6.5 Hz), 133.66 (s), 133.07 (d, J = 10.7 Hz), 131.44 (s), 130.57 (s), 130.43 (s), 129.59 (s), 129.47 (s), 129.35 (s), 129.11 (d, J = 2.9 Hz), 128.80 (d, J = 2.9 Hz), 128.64 (s), 128.50 (s), 126.51 (s), 125.93 (s), 123.22 (s), 120.51 (s), 117.47 (s), 115.61 (s), 105.58 (s), 104.43 (s), 57.24 (d, J = 8.1 Hz), 56.86 (s), 55.79 (s).

Preparation of Ni5. Similar procedure was employed except **L5** (302 mg, 0.5 mmol) was used. **Ni5** was obtained as a bright yellow solid (1.2 g, 77%). ^{1}H NMR (400 MHz, CDCl$_3$) δ 7.61 (s, 8H), 7.43 (s, 1H), 7.42 (s, 4H), 7.40–7.23 (m, 6H), 7.20 (s, 1H), 7.10 (s, 1H), 7.07 m, 2H), 6.92 (m, 1H), 6.82–6.61 (m, 3H), 6.53 (s, 0.5H), 6.46–6.28 (m, 1H), 5.20 (s, 0.5H), 4.91 (d, J = 5.4 Hz, 0.5H), 4.75 (s, 0.5H), 4.34 (d, J = 5.8 Hz, 1H), 4.10 (d, J = 23.8 Hz, 1H), 3.92 (s, 0.5H), 3.63 (dd, J = 29.7, 16.2 Hz, 6H), 2.26 (d, J = 10.6 Hz, 0.5H), 1.94 (s, 0.5H), 1.71 (s, 0.5H), 1.56–1.38 (m, 3H), 1.31 (d, J = 14.7 Hz, 3H), 1.08 (d, J = 6.1 Hz, 3H), 0.55 (d, J = 28.5 Hz, 3H). ^{31}P NMR (162 MHz, CDCl$_3$) δ 70.06 (dd, J = 96.4, 24.3 Hz), 18.60 (dd, J = 236.6, 96.3 Hz). ^{13}C NMR (101 MHz, CDCl$_3$) δ 161.76 (dd, J = 99.7, 49.9 Hz), 158.06 (d, J = 49.7 Hz), 136.01 (s), 134.84 (s), 133.50 (s), 132.97 (s), 131.26 (s), 130.63 (s), 130.47 (s), 130.36 (s), 129.28 (s), 129.08 (s), 128.82 (s), 128.57 (d, J = 16.9 Hz), 128.49 (s), 126.51 (s), 125.95 (s), 123.24 (s), 120.53 (s), 117.48 (s), 115.41 (s), 105.63 (s), 104.42 (s), 57.17 (s), 55.79 (s), 47.35 (d, J = 51.8 Hz), 31.59 (s), 24.76–23.05 (m), 22.44 (d, J = 42.6 Hz), 14.06 (s).

3.4. Polymerization

Procedure for the homopolymerization of ethylene. In a typical experiment, a 350 mL glass thick-walled pressure vessel was charged with toluene (18 mL) and a magnetic stir bar in a glovebox. The pressure vessel was connected to a high-pressure line and the solution was degassed. The vessel was warmed to 80 °C using an oil bath (water bath for polymerizations at room temperature) and allowed to equilibrate for 15 min. The desired amount of the Pd or Ni complex in CH_2Cl_2 (2 mL) was injected into the polymerization system via syringe. With rapid stirring, the reactor was pressurized with ethylene, which was maintained at 8.0 atm. After the desired amount of time, the pressure vessel was vented and the polymer was precipitated in acidified methanol (methanol/HCl = 50/1) and dried at 50 °C for 24 h under vacuum.

Procedure for the copolymerization of ethylene and polar monomers. In a typical experiment, a 350 mL glass thick-walled pressure vessel was charged with a magnetic stir bar, toluene, and the polar monomer (18 mL total volume) in a glovebox. The pressure vessel was connected to a high-pressure line and the solution was degassed. The vessel was warmed to 80 °C using an oil bath and allowed to equilibrate for 15 min. The metal complex (20 μmol) in CH_2Cl_2 (2 mL) was injected into the polymerization system via syringe. With rapid stirring, the reactor was pressurized with ethylene, which was maintained at 8.0 atm. After 6 h, the pressure vessel was vented and the polymer was precipitated in acidified methanol (methanol/HCl = 50/1) and dried at 50 °C for 24 h under vacuum.

3.5. Computational method

All the DFT calculations were performed with the Gaussian 16 program [69]. The B3LYP hybrid exchange-correlation functional was used for geometry optimizations [70]. For **Pd1′**, **Pd2′**, **Pd3′**, and **Pd-Ph′**, the 6-31G(d,p) basis set was used for H, C, N, O, P and Cl atoms. Pd atoms were treated by the LANL2DZ basis set. For **Ni2′**, **Ni-Ph′**, **Ni4′**, and **Ni5′**, the 6–31 + G(d,p) basis set was used for H, C, N, O, and P atoms. Ni atoms were treated by the LANL2DZ basis set [71,72]. Normal modes of all structures were examined. No imaginary frequency was observed.

4. Conclusions

In summary, a series of PNPO-type phosphinoamine phosphoramidate/phosphoramide ligands and the corresponding palladium and nickel catalysts have been designed, synthesized, characterized and investigated in ethylene polymerization and copolymerization of ethylene with various polar monomers. The palladium and nickel complexes exhibited high activities in ethylene (co) polymerization and generated high-molecular-weight polyethylene and functionalized polyethylene. Most interestingly, the introduction of electron-donating substituents in these palladium complexes can significantly increase polymer molecular weight while maintaining high (co)polymerization activity. For the nickel case, the catalysts bearing less electronic donating substituents resulted in higher catalytic activities in ethylene polymerization and copolymerization reactions, indicating beneficial effects though the reduction of the electron density from the Ni center. This study provides insights for future designing of high performance transition metal catalyst for ethylene polymerization and copolymerization with polar comonomers.

Declaration of Competing Interest

The authors declare that they have no known competing financial interests or personal relationships that could have appeared to influence the work reported in this paper.

Acknowledgements

This work was supported by National Natural Science Foundation of China (NSFC, 22001004 and GG2060200138).

Appendix A. Supplementary material

Supplementary data to this article can be found online at https://doi.org/10.1016/j.jcat.2020.11.023.

References

[1] M. Stürzel, S. Mihan, R. Mulhaupt, From multisite polymerization catalysis to sustainable materials and all-polyolefin composites, Chem. Rev. 116 (2016) 1398–1433.
[2] T.C. Chung, Functionalization of polyolefins, Academic Press, San Diego, CA, 2002.
[3] J.Y. Dong, Y. Hu, Design and synthesis of structurally well-defined functional polyolefins via transition metal-mediated olefin polymerization chemistry, Coord. Chem. Rev. 250 (2005) 47–65.
[4] T. Rünzi, S. Mecking, Saturated polar-substituted polyethylene elastomers from insertion polymerization, Adv. Funct. Mater. 24 (2014) 387–395.
[5] S. Dai, C. Chen, Palladium-catalyzed direct synthesis of various branched, carboxylic acid-functionalized polyolefins: characterization, derivatization, and properties, Macromolecules 51 (2018) 6818–6824.
[6] Y. Na, S. Dai, C. Chen, Direct synthesis of polar-functionalized Linear LowDensity Polyethylene (LLDPE) and Low-Density Polyethylene (LDPE), Macromolecules 51 (2018) 4040–4048.
[7] P. Xiang, Z.B. Ye, Hyperbranched polyethylene ionomers containing cationic tetralkylammonium ions synthesized by Pd-diimine-catalyzed direct ethylene copolymerization with ionic liquid comonomers, Macromolecules 48 (2015) 6096–6107.
[8] C. Zou, C. Chen, Polar-functionalized, crosslinkable, self-healing and photoresponsive polyolefins, Angew. Chem. Int. Ed. 59 (2020) 395–402.
[9] Y. Na, C. Chen, Catechol functionalized polyolefins, Angew. Chem. Int. Ed. 59 (2020) 7953–7959.
[10] S. Dai, S. Li, G. Xu, C. Chen, Direct synthesis of polar functionalized polyethylene thermoplastic elastomer, Macromolecules 53 (2020) 2539–2546.
[11] J. Gao, W. Cai, Y. Hu, C. Chen, Improving the flame retardancy of polyethylenes through palladium-catalyzed incorporation of polar comonomers, Poly. Chem. 10 (2019) 1416–1422.
[12] A. Keyes, A.H. Basbug, E. Ordonez, U. Ha, D.B. Beezer, H. Dau, Y.S. Liu, E. Tsogtgerel, G.R. Jones, E. Harth, Olefins and vinyl polar monomers: bridging the gap for next generation materials, Angew. Chem. Int. Ed. 58 (2019) 12370–12391.
[13] C. Tan, C. Chen, Emerging palladium and nickel catalysts for copolymerization of olefins with polar monomers, Angew. Chem. Int. Ed. 58 (2019) 7192–7200.
[14] S.D. Ittel, L.K. Johnson, M. Brookhart, Late-metal catalysts for ethylene homo- and copolymerization, Chem. Rev. 100 (2000) 1169–1204.
[15] J.A. Gladysz, Z.T. Ball, G. Bertrand, S.A. Blum, V.M. Dong, R. Dorta, F.E. Hahn, M. G. Humphrey, W.D. Jones, J. Klosin, I. Manners, T.J. Marks, J.M. Mayer, B. Rieger, J.C. Ritter, A.P. Sattelberger, J.M. Schomaker, V.-W.-W. Yam, Organometallics Roundtable 2011, Organometallics 31 (2012) 1–18.
[16] L.K. Johnson, C.M. Killian, M. Brookhart, New Pd(II)- and Ni(II)-based catalysts for polymerization of ethylene and alpha.-olefins, J. Am. Chem. Soc. 117 (1995) 6414–6415.
[17] L.K. Johnson, S. Mecking, M. Brookhart, Copolymerization of ethylene and propylene with functionalized vinyl monomers by palladium(II) catalysts, J. Am. Chem. Soc. 118 (1996) 267–268.
[18] Z. Chen, M. Brookhart, Exploring ethylene/polar vinyl monomer copolymerizations using Ni and Pd α-diimine catalysts, Acc. Chem. Res. 51 (2018) 831–1839.
[19] D.J. Walsh, M.G. Hyatt, S.A. Miller, D. Guironnet, Recent trends in catalytic polymerizations, ACS Catal. 9 (2019) 11153–11188.
[20] C. Tan, C. Chen, Nickel catalysts for the synthesis of ultra-high molecular weight polyethylene, Sci. Bull. 65 (2020) 1137–1138.
[21] Y. Zhang, C. Wang, S. Mecking, Z. Jian, Angew. Chem. Int. Ed. 59 (2020) 14296–14302.
[22] S. Dai, C. Chen, A self-supporting strategy for gas-phase and slurry-phase ethylene polymerization using late-transition-metal catalysts, Angew. Chem. Int. Ed. 59 (2020) 14884–14890.
[23] Q. Muhammad, C. Tan, C. Chen, Concerted steric and electronic effects on α-diimine nickel- and palladium-catalyzed ethylene polymerization and copolymerization, Sci. Bull. 65 (2020) 300–307.
[24] C. Hong, X. Wang, C. Chen, Macromolecules 52 (2019) 7123–7129.
[25] C. Tan, W. Pang, C. Chen, A phenol-containing α-diimine ligand for nickel- and palladium-catalyzed ethylene polymerization, Chinese J. Polym. Sci. 37 (2019) 974–980.
[26] X. Hu, C. Wang, Z. Jian, Comprehensive studies of the ligand electronic effect on unsymmetrical α-diimine nickel(ii) promoted ethylene (co) polymerizations, Polym. Chem. 11 (2020) 4005–4012.
[27] G. Wang, D. Peng, Y. Sun, C. Chen, Interplay of supramolecular chemistry and photochemistry with palladium-catalyzed ethylene polymerization, CCS Chem. 2 (2020), https://doi.org/10.31635/ccschem.020.202000414.
[28] M. Li, X. Wang, Y. Luo, C. Chen, A second-coordination-sphere strategy to modulate nickel- and palladium-catalyzed olefin polymerization and copolymerization, Angew. Chem. Int. Ed. 56 (2017) 11604–11609.
[29] L. Zhong, C. Du, G. Liao, H. Liao, H. Zheng, Q. Wu, H. Gao, Effects of backbone substituent and intra-ligand hydrogen bonding interaction on ethylene polymerizations with α-diimine nickel catalysts, J. Catal. 375 (2019) 113–123.

[30] L. Zhong, H. Zheng, C. Du, W. Du, G. Liao, C.S. Cheung, H. Gao, Thermally robust α-diimine nickel and palladium catalysts with constrained space for ethylene (co)polymerizations, J. Catal. 384 (2020) 208–217.

[31] F.-S. Liu, H.-B. Hu, Y. Xu, L.-H. Guo, S.-B. Zai, K.-M. Song, H.-Y. Gao, L. Zhang, F.-M. Zhu, Q. Wu, Thermostable α-Diimine Nickel(II) catalyst for ethylene polymerization: effects of the substituted backbone structure on catalytic properties and branching structure of polyethylene, Macromolecules 42 (2009) 7789–7796.

[32] L. Guo, H. Gao, Q. Guan, H. Hu, J. Deng, J. Liu, F. Liu, Q. Wu, Substituent effects of the backbone in α-diimine palladium catalysts on homo- and copolymerization of ethylene with methyl acrylate, Organometallics 31 (2012) 6054–6062.

[33] L. Zhong, G. Li, G. Liang, H. Gao, Q. Wu, Enhancing thermal stability and living fashion in α-diimine–nickel-catalyzed (co)polymerization of ethylene and polar monomer by increasing the steric bulk of ligand backbone, Macromolecules 50 (2017) 2675–2682.

[34] S. Zhong, Y. Tan, L. Zhong, J. Gao, H. Liao, L. Jiang, H. Gao, Q. Wu, Precision synthesis of ethylene and polar monomer copolymers by palladium-catalyzed living coordination copolymerization, Macromolecules 50 (2017) 5661–5669.

[35] E. Drent, R. van Dijk, R. van Ginkel, B. van Oort, R.I. Pugh, Palladium catalysed copolymerisation of ethene with alkylacrylates: polar comonomer built into the linear polymer chain, Chem. Commun. (2002) 744–745.

[36] A. Nakamura, S. Ito, K. Nozaki, Coordination-insertion copolymerization of fundamental polar monomers, Chem. Rev. 109 (2009) 5215–5244.

[37] A. Nakamura, T.M.J. Anselment, J. Claverie, B. Goodall, R.F. Jordan, S. Mecking, B. Rieger, A. Sen, P.W.N.M. van Leeuwen, K. Nozaki, Ortho-phosphinobenzenesulfonate: a superb ligand for palladium-catalyzed coordination-insertion copolymerization of polar vinyl monomers, Acc. Chem. Res. 46 (2013) 1438–1449.

[38] S. Ito, Palladium-catalyzed homo- and copolymerization of polar monomers: synthesis of aliphatic and aromatic polymers, Bull. Chem. Soc. Jpn. 91 (2018) 251–261.

[39] N. Schuster, T. Rünzi, S. Mecking, Reactivity of functionalized vinyl monomers in insertion copolymerization, Macromolecules 49 (2016) 1172–1179.

[40] M. Chen, C. Chen, Direct and tandem routes for the copolymerization of ethylene with polar functionalized internal olefins, Angew. Chem. Int. Ed. 59 (2020) 1206–1210.

[41] C. Tan, M. Qasim, W. Pang, C. Chen, Ligand-metal secondary interaction in phosphine-sulfonate palladium and nickel catalyzed ethylene (co) polymerization, Polym. Chem. 11 (2020) 411–416.

[42] L. Cui, M. Chen, C. Chen, D. Liu, Z. Jian, Systematic studies on (co) polymerization of polar styrene monomers with palladium catalysts, Macromolecules 52 (2019) 7197–7206.

[43] J. Xia, Y. Zhang, J. Zhang, Z. Jian, High-performance neutral phosphine-sulfonate nickel(II) catalysts for efficient ethylene polymerization and copolymerization with polar monomers, Organometallics 38 (2019) 1118–1126.

[44] F.W. Seidel, I. Tomizawa, K. Nozaki, Expedient synthetic identification of a novel P-stereogenic ligand motif for the palladium-catalyzed preparation of isotactic polar polypropylenes, Angew. Chem. Int. Ed. 59 (2020), https://doi.org/10.1002/anie.202009027.

[45] B. Neuwald, L. Caporaso, L. Cavallo, S. Mecking, Concepts for stereoselective acrylate insertion, J. Am. Chem. Soc. 135 (2013) 1026–1036.

[46] Y. Ota, S. Ito, M. Kobayashi, S. Kitade, K. Sakata, T. Tayano, K. Nozaki, Crystalline isotactic polar polypropylene from the palladium-catalyzed copolymerization of propylene and polar monomers, Angew. Chem. Int. Ed. 55 (2016) 7505–7509.

[47] B.P. Carrow, K. Nozaki, Synthesis of functional polyolefins using cationic bisphosphine monoxide-palladium complexes, J. Am. Chem. Soc. 134 (2012) 8802–8805.

[48] X. Sui, S. Dai, C. Chen, Ethylene polymerization and copolymerization with polar monomers by cationic phosphine phosphonic amide palladium complexes, ACS Catal. 5 (2015) 5932–5937.

[49] W. Zhang, P.M. Waddell, M.A. Tiedemann, C.E. Padilla, J.J. Mei, L.Y. Chen, B.P. Carrow, Electron-rich metal cations enable synthesis of high molecular weight, linear functional polyethylenes, J. Am. Chem. Soc. 140 (2018) 8841–8850.

[50] N.D. Contrella, J.R. Sampson, R.F. Jordan, Copolymerization of ethylene and methyl acrylate by cationic palladium catalysts that contain phosphine-diethyl phosphonate ancillary ligands, Organometallics 33 (2014) 3546–3555.

[51] M. Chen, C. Chen, A versatile ligand platform for palladium- and nickel-catalyzed ethylene copolymerization with polar monomers, Angew. Chem. Int. Ed. 57 (2018) 3094–3098.

[52] M. Xu, F. Yu, P. Li, G. Xu, S. Zhang, F. Wang, Enhancing chain initiation efficiency in the cationic allyl-nickel catalyzed (co)polymerization of ethylene and methyl acrylate, Inorg. Chem. 59 (2020) 4475–5448.

[53] C. Fliedel, A. Ghisolfi, P. Braunstein, Functional short-bite ligands: synthesis, coordination chemistry, and applications of N-functionalized bis (diaryl/dialkylphosphino)amine-type ligands, Chem. Rev. 116 (2016) 9237–9304.

[54] R.E. Black, R.F. Jordan, Synthesis and reactivity of palladium(II) alkyl complexes that contain phosphine-cyclopentanesulfonate ligands, Organometallics 36 (2017) 3415–3428.

[55] C. Hansch, A. Leo, R.W. Taft, A survey of Hammett substituent constants and resonance and field parameters, Chem. Rev. 91 (1991) 165–195.

[56] K. Gholivand, Mahzouni, H. Reza, Electronic and steric effects of substituents on the conformational diversity and hydrogen bonding of N-(4-X-phenyl)-N′, N″-bis(piperidinyl) phosphoric triamides (X = F, Cl, Br, H, CH3): A combined experimental and DFT study, Polyhedron 30 (2011) 61–69.

[57] K. Gholivand, H. Mahzouni, M. Reza, S. Pourayoubi, Amiri, High-coordinated lanthanum(III) complexes with new mono- and bidentate phosphoryl donors; spectroscopic and structural aspects, Inorg. Chim. Acta 363 (2010) 2318–2324.

[58] H.R. Barai, Concerted pathway to the mechanism of the anilinolysis of bis(N, N-diethylamino)phosphinic chloride in acetonitrile, Aust. J. Chem. 70 (2017) 101–105.

[59] X. Chen, Z. Xiao, H. Chu, B. Wang, A. Peng, Reinvestigation of the iodine-mediated phosphoramidation reaction of amines and P(OR)3 and its synthetic applications, Org. Biomol. Chem. 16 (2018) 6783–6790.

[60] T. Rünzi, U. Tritschler, P. Roesle, I. Göttker-Schnetmann, H.M. Möller, L. Caporaso, A. Poater, L. Cavallo, S. Mecking, Activation and deactivation of neutral palladium(II) phosphinesulfonato polymerization catalysts, Organometallics 31 (2012) 8388–8406.

[61] C.S. Popeney, Z.B. Guan, Effect of ligand electronics on the stability and chain transfer rates of substituted Pd(II) R-diimine catalysts, Macromolecules 43 (2010) 4091–4097.

[62] P. Wucher, V. Goldbach, S. Mecking, Organometallics 32 (2013) 4516–4522.

[63] L. Guo, W. Sun, S. Li, G. Xu, S. Dai, Bulky yet flexible substituents in insertion polymerization with α-diimine nickel and palladium systems, Polym. Chem. 10 (2019) 4866–4871.

[64] S. Dai, S. Li, G. Xu, C. Wu, Y. Liao, L. Guo, Flexible cycloalkyl substituents in insertion polymerization with α-diimine nickel and palladium species, Polym. Chem. 11 (2020) 1393–1400.

[65] J.L. Rhinehart, L.A. Brown, B.K. Long, A robust Ni(II) α-diimine catalyst for high temperature ethylene polymerization, J. Am. Chem. Soc. 135 (2013) 16316–16319.

[66] J. Gao, B. Yang, C. Chen, Sterics versus electronics: Imine/phosphine-oxide-based nickel catalysts for ethylene polymerization and copolymerization, J. Catal. 369 (2019) 233–238.

[67] G. Wang, M. Li, W. Pang, M. Chen, C. Tan, Lewis acids in situ modulate pyridazine-imine Ni catalysed ethylene (co)polymerisation, New J. Chem. 43 (2019) 13630–13634.

[68] L. Falivene, Z. Cao, A. Petta, L. Serra, A. Poater, R. Oliva, V. Scarano, L. Cavallo, Towards the online computer-aided design of catalytic pockets, Nat. Chem. 11 (2019) 872–879.

[69] M. J. Frisch, G. W. Trucks, H. B. Schlegel, G. E. Scuseria, M. A. Robb, J. R. Cheeseman, G. Scalmani, V. Barone, G. A. Petersson, H. Nakatsuji, X. Li, M. Caricato, A. V. Marenich, J. Bloino, B. G. Janesko, R. Gomperts, B. Mennucci, H. P. Hratchian, J. V. Ortiz, A. F. Izmaylov, J. L. Sonnenberg, D. Williams-Young, F. Ding, F. Lipparini, F. Egidi, J. Goings, B. Peng, A. Petrone, T. Henderson, D. Ranasinghe, V. G. Zakrzewski, J. Gao, N. Rega, G. Zheng, W. Liang, M. Hada, M. Ehara, K. Toyota, R. Fukuda, J. Hasegawa, M. Ishida, T. Nakajima, Y. Honda, O. Kitao, H. Nakai, T. Vreven, K. Throssell, J. A. Montgomery, Jr., J. E. Peralta, F. Ogliaro, M. J. Bearpark, J. J. Heyd, E. N. Brothers, K. N. Kudin, V. N. Staroverov, T. A. Keith, R. Kobayashi, J. Normand, K. Raghavachari, A. P. Rendell, J. C. Burant, S. S. Iyengar, J. Tomasi, M. Cossi, J. M. Millam, M. Klene, C. Adamo, R. Cammi, J. W. Ochterski, R. L. Martin, K. Morokuma, O. Farkas, J. B. Foresman, and D. J. Fox, Gaussian, Inc., Wallingford CT, 2016.

[70] A.D. Becke, Density-functional thermochemistry. 3. The role of exact exchange, J. Chem. Phys. 98 (1993) 5648–5652.

[71] R. Krishnan, J.S. Binkley, R. Seeger, J.A. Pople, Self-consistent molecular-orbital methods. 20. Basis set for correlated wave-functions, J. Chem. Phys. 72 (1980) 650–654.

[72] A.V. Marenich, C.J. Cramer, D.G. Truhlar, Universal solvation model based on solute electron density and on a continuum model of the solvent defined by the bulk dielectric constant and atomic surface tensions, J. Phys. Chem. B 113 (2009) 6378–6396.